



Universiteit
Leiden
The Netherlands

Formation of graphene and hexagonal boron nitride on Rh(111) studied by in-situ scanning tunneling microscopy

Dong, G.

Citation

Dong, G. (2012, November 7). *Formation of graphene and hexagonal boron nitride on Rh(111) studied by in-situ scanning tunneling microscopy*. *Casimir PhD Series*. Kamerlingh Onnes Laboratory, Leiden Institute of Physics, Faculty of Science, Leiden University. Retrieved from <https://hdl.handle.net/1887/20105>

Version: Corrected Publisher's Version

License: [Licence agreement concerning inclusion of doctoral thesis in the Institutional Repository of the University of Leiden](#)

Downloaded from: <https://hdl.handle.net/1887/20105>

Note: To cite this publication please use the final published version (if applicable).

Cover Page



Universiteit Leiden



The handle <http://hdl.handle.net/1887/20105> holds various files of this Leiden University dissertation.

Author: Dong, Guocai

Title: Formation of graphene and hexagonal boron nitride on Rh(111) studied by in-situ scanning tunneling microscopy

Date: 2012-11-07

Chapter 5 Adsorption and decomposition of borazine

5.1 The breaking of B-N bonds

The observation of two different types of island edges implies that B-N bonds are broken at the growth temperature. This is illustrated in Fig. 5.1, which shows that even though it is technically possible to construct a layer of *h*-BN without breaking the B-N bonds in the deposited borazine molecules, the edges of the resulting islands would all be equivalent, terminated by both B- and N-atoms (the outer contour of the island in Fig. 5.1. Different edges, e.g. terminated exclusively by either B-atoms or N-atoms, can only be obtained by interrupting the layer along another direction, as indicated by the red line in Fig. 5.1. Such a termination had already been suggested for BN-islands on Ni(111) [24]. This edge direction is further supported by the observed orientation of the nanomesh pattern in the islands. This can be concluded from a comparison with the atomically resolved images of the nanomesh structure and with supporting theory, in refs. [11, 14]. An *h*-BN island, with a straight edge along the direction of the red line in Fig. 5.1, cannot be created by combining the (BN)₃ rings of the borazine molecules, as building blocks. The breaking of the B-N bonds forms a necessary step in the process. The observed, compact island shapes is an indication of the B-N bond decomposition. This step probably requires a high temperature, as is suggested by the aggregates observed in Fig. 4.2A. These only started rearranging into compact shapes, with the preferred edge orientations (Fig. 4.2B), at temperatures between 762 K and 806 K.

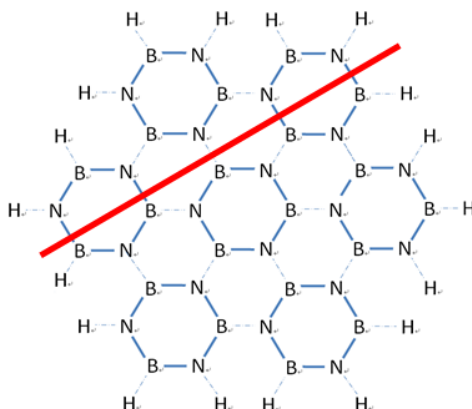


Fig. 5.1 Sketch indicating how an *h*-BN overlayer can be formed without breaking the B-N bonds, by combining the intact (BN)₃ rings originating from the borazine molecules. The solid blue lines denote the bonds in the original molecules; the dashed ones are new, and have formed in combination with the loss of hydrogen. The solid red line shows that only by cutting the B-N bonds the island develop can two different types of edges, as seen in the STM images (e.g. Fig. 4.4) either N- or B-terminated.

5.2 Desorption of borazine molecules and B and N atoms

In section 4.3 it was already mentioned that, after a borazine exposure at a temperature of 672 K a pressure of 3.7×10^{-10} mbar for 10 minutes, no change was detected on the Rh surface. The same exposure at room temperature gave a very noticeable structure. Only when the pressure of the borazine was increased to 1.5×10^{-9} mbar, small islands were formed on the surface. The complete absence of borazine or BN islands on the surface at the lower pressure requires desorption of borazine molecules under those conditions. The density of borazine on the surface must have remained at an equilibrium value that was a function of the borazine pressure. Only when this density exceeded a critical value, as was the case at the higher borazine pressure, nucleation of the *h*-BN islands started, and further deposited borazine could attach onto the newly formed islands. The consumption of borazine by the BN growth must have reduced the density of borazine molecules on the surface.

A similar scenario must apply to B and N adatoms. At a higher temperature of 978 K, a clean Rh surface was first exposed to $\sim 5 \times 10^{-9}$ mbar of borazine for 3 minutes, which did not result in deposition of either borazine or *h*-BN on the surface. An exposure to a higher borazine pressure of 5×10^{-8} mbar for 3 minutes resulted in nucleation at a density of $3/\mu\text{m}^2$. As we had concluded before, borazine had already decomposed at this temperature. This must also have been the case during the lower-pressure exposure. The absence of nucleation at the lower pressure then implies that the fragments of the borazine molecule, i.e. either separate B and N adatoms or BN-units, can also desorb from the Rh(111) surface at 978 K.

5.3 From which borazine is the *h*-BN overlayer formed?

In the previous section we have learned that borazine molecules as well as B and N adatoms can desorb from the metal surface. In this section, we investigate which landing sites of the borazine molecules contribute to the growth of the *h*-BN. The method consists of measuring the rate at which vacancy islands in the *h*-BN overlayer fill up. We can safely assume that the chemical potential, or the density of B and N atoms inside a vacancy island, is uniform, as long as the geometry of the island is not so complex that it would influence the diffusion of the surface species. When we assume that only those borazine molecules that land on the bare metal surface can stick decompose and contribute to the formation of *h*-BN, the time dependence of the total area of the vacancy island can be calculated to satisfy:

$$\frac{dA}{dt} = -\frac{A}{D} I \lambda = \frac{A}{D} \lambda \frac{P}{\sqrt{2\pi m k_b T}} = -\alpha A P \lambda \quad \text{Eq. 5.1}$$

Here, A is the area of the vacancy island; P is the impinging borazine pressure. t is in seconds; λ represents the efficiency effective number of the B and the N atoms from the borazine contributing to the *h*-BN overlayer per impinging borazine molecule. D represents the areal density of B and N atoms in the *h*-BN overlayer and the impingement rate of ethylene I is expressed in terms of the borazine gas pressure P , the (gas) temperature T , and the mass m of a borazine molecule, using standard kinetic gas

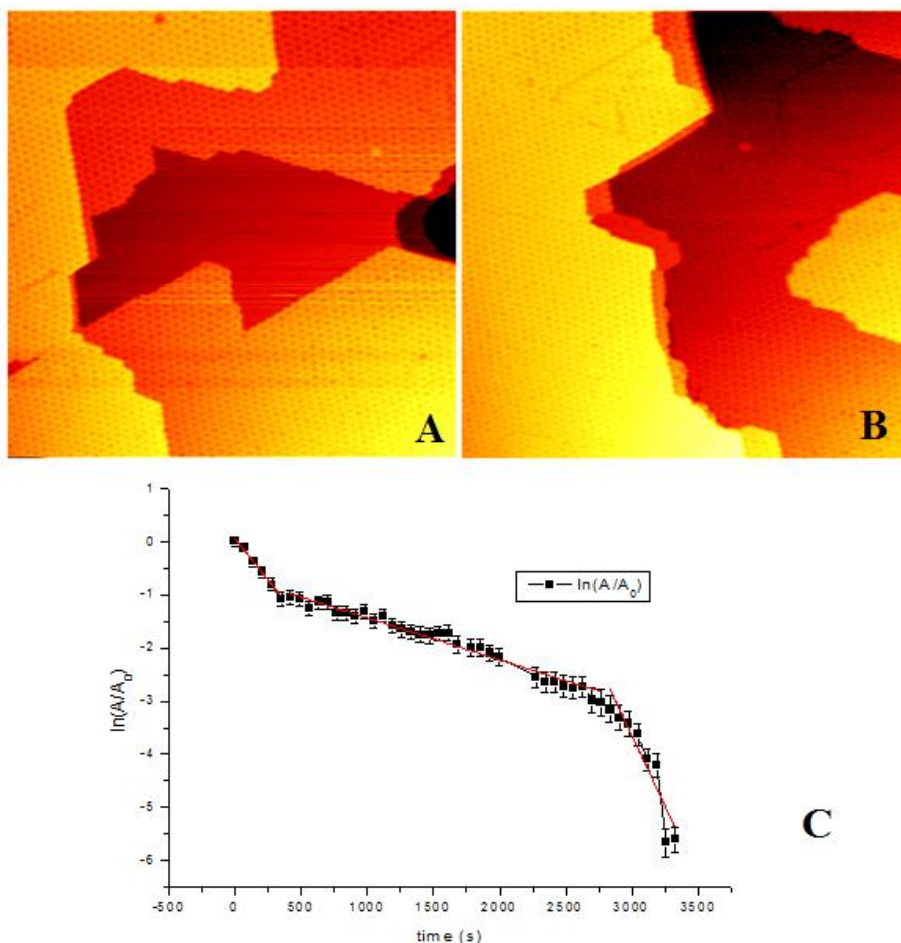


Fig. 5.2 STM images ($170 \times 170 \text{ nm}^2$) at the beginning (A) and end (B) of the filling up of a vacancy island in a *h*-BN overlayer on Rh(111) at a sample temperature of 978 K. The borazine pressure in the vacuum chamber was 3.2×10^{-9} mbar. (C) Time dependence of the area of the vacancy island, relative to the area in image (A). The slopes of the three linear fits to the early, intermediate and late stages of the process are $-3.1 \times 10^{-3} \text{ s}^{-1}$, $-0.79 \times 10^{-3} \text{ s}^{-1}$ and $-5.1 \times 10^{-3} \text{ s}^{-1}$ respectively, corresponding to λ -values of 4.6, 1.2, and 7.6 in Eq. 5.2. As argued in the text, the values that exceed 3 indicate that a significant supply of B and N atoms originates from the lower Rh terrace to which the vacancy island is connected.

theory. The part that has surely remained unchanged during deposition has been combined in the constant α . Based on this differential equation, we expect exponential decay of the uncovered area. Solving this differential equation, we obtain:

$$\ln\left(\frac{A}{A_0}\right) = \alpha P \lambda t \quad \text{Eq. 5.2}$$

Before testing this prediction experimentally, we first calibrated the relation between the measured borazine pressure and the impinging flux of borazine molecules, by exposing a clean Rh surface to a low dose of 2.1×10^{-7} mbar s of borazine at room temperature. We trust that this temperature is low enough to disable decomposition and desorption of the deposited molecules and we assume the resulting coverage to be low enough to avoid reflection of borazine molecules impinging on other borazine molecules. From the coverage of adsorbed borazine molecules visible in the STM image we obtain $\alpha = 2.1 \times 10^5$ an impingement rate on Rh(111) equivalent to 0.65 monolayers of *h*-BN per 10^{-6} mbar s of borazine exposure, where 1 monolayer is defined as a completely filled *h*-BN overlayer. Armed with this calibration, the λ -factor in Eq. 5.2 can be accurately calculated.

We discuss the analysis of the area of the four vacancy islands, shown in Fig. 5.2, Fig. 5.3 and Fig. 5.4. The data in the first two figures were extracted from the experiment at 978 K, discussed above, while the data in Fig. 5.4 had been measured at a somewhat lower temperature of 865 K. Each of the figures shows the first and last images of the episodes that have been analyzed and the graph in each figure is a semilogarithmic plot of the relative area of vacancy islands. The two plots in Fig. 5.4 are for the two vacancy islands in the field of view. The prediction of Eq. 5.2 should result in straight lines in these plots, with a negative slope from which the value of λ can be determined directly. Even though we can fit straight lines to the four semilogarithmic area-versus-time plots, three of the curves deviate noticeably from linear behavior and become steeper towards the end.

5.3 From which borazine is the h-BN overlayer formed?

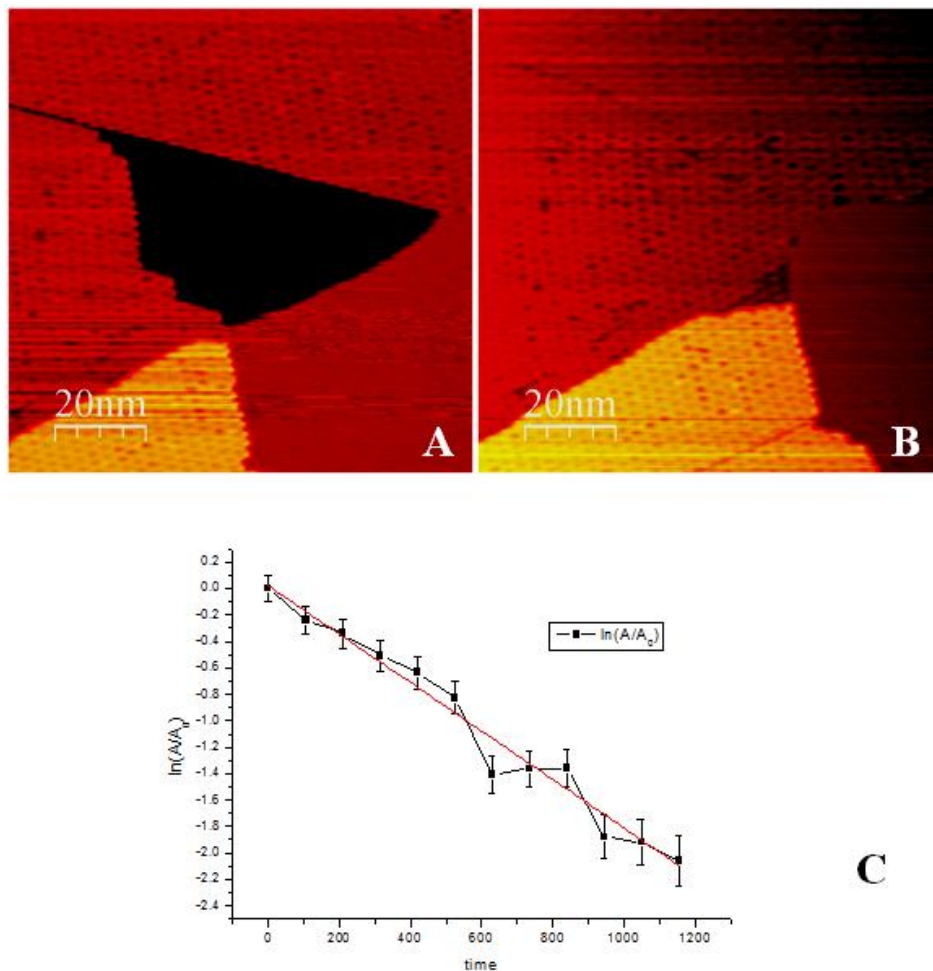


Fig. 5.3 STM images ($100 \times 100 \text{ nm}^2$) at the beginning (A) and end (B) of the filling up of a vacancy island in an h-BN overlayer on Rh(111) at a sample temperature of 978 K. The borazine pressure in the vacuum chamber was 1.5×10^{-9} mbar. (C) Time dependence of the area of the vacancy island, relative to the area in image (A). The slope of the linear fit of $-1.8 \times 10^{-3} \text{ s}^{-1}$ corresponds to a λ -value of 5.7 in Eq. 5.2. As argued in the text, this value, which is higher than 3, indicates that a significant supply of B and N atoms originates from the higher Rh terrace on the right, to which the vacancy island is connected.

The λ -values obtained from the straight-line fits to the data in Fig. 5.2 and Fig. 5.3 are higher than 3, namely 4.6 and 7.6 for the initial and late stages in Fig. 5.2 and 5.7 for the entire fit in Fig. 5.3C. We ascribe these high values to the fact that the two vacancy islands in these figures were both connected to a part of the bare Rh surface that was either one atomic layer higher or lower, of which the area had not been counted as part of the vacancy island. We had initially assumed exchange of B and N between the two Rh levels to be strongly suppressed, but the high λ -values indicate that both vacancy islands had been filling up with a significant supply of B and N from the other Rh level.

The two vacancy islands in Fig. 5.4 were both fully enclosed by the *h*-BN overlayer, so that for these vacancy islands there had been no additional sources of B or N atoms. If we fit straight lines to the area plots for these two islands, we indeed find λ -values below 3, namely 1.2 for the upper island and 1.0 for the lower one. As already mentioned, both plots curve downward. The slopes of the final parts of both curves correspond to λ -values of 3.0, indicating that only in the final stages, when the vacancy islands are close to being filled completely, all B and N atoms from the borazine molecules that impinge on the remaining bare Rh ‘enclaves’ get fully incorporated into the *h*-BN overlayer. The fact that the two curves start out with much more modest slopes shows that in larger vacancy islands, a significant fraction of the supplied borazine molecules (or B and N atoms) is desorbed rather than incorporated. The corresponding finite residence time of the diffusing surface species – adsorbed borazine or B and N adatoms – implies that it can only reach the edge of the vacancy island over a finite distance. In other words, there is a finite, effective capture zone inside the contour of each vacancy island. Borazine impinging within this zone is fully incorporated at the edge and contributes to the filling up of the vacancy island, whereas borazine that impinges on the Rh but closer to the center, i.e. outside the capture zone, is destined to desorb. This scenario naturally explains the curvature of the measured area plots and suggests that we should modify the expected growth law according to:

$$\frac{dA}{dt} = -3\alpha wLP \quad \text{Eq. 5.3}$$

Here, L is the length of the inner contour of the vacancy and w is the width of the capture zone, which is determined by the diffusion coefficient and the residence time and should therefore depend on the substrate temperature. From this we obtain:

$$A(t) = A_0 - 3awP \int_{t_0}^t L(t) dt \quad \text{Eq. 5.4}$$

We can check the validity of Eq. 5.4 by integrating it numerically. The only free fitting parameter is then the width w of the capture zone. The result of this procedure for the upper and lower vacancy islands of Fig. 5.4 is shown by the blue dots in panels C and D. The best-fit values of w are 0.8 nm and 1 nm respectively. For both vacancy islands, this simple model provides an excellent description of the way they fill up as a function of time. The fact that the best-fit values of capture zone widths are nearly identical provides extra confidence that the Eq. 5.3 provides a meaningful description of the process. The capture zone width is surprisingly small, which shows that at 865 K, most of the borazine that impinges on the Rh(111) surface desorbs already within a small number of diffusion steps on the surface.

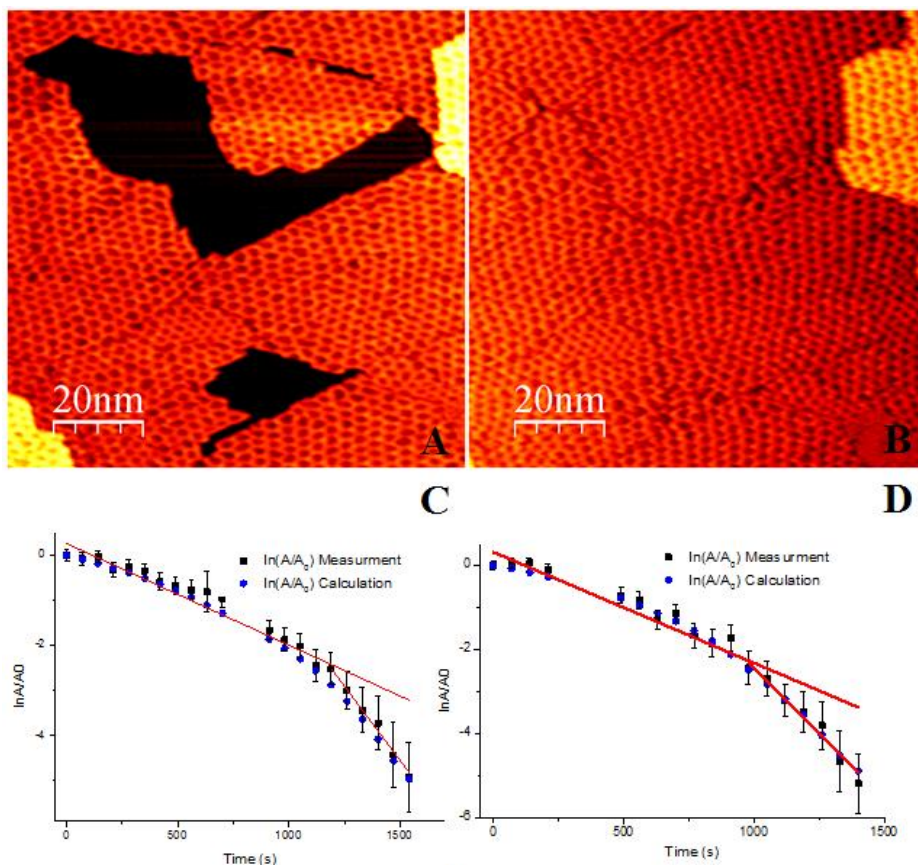


Fig. 5.4 STM images ($100 \times 100 \text{ nm}^2$) at the beginning (A) and end (B) of the filling up of two vacancy islands in an *h*-BN overlayer on Rh(111) at a sample temperature of 865 K. The borazine pressure in the vacuum chamber was 1.0×10^{-8} mbar. In (C) and (D), the black squares are the time-dependent areas measured directly from the images for the upper and lower vacancy islands, relative to their starting sizes in image (A). The linear fits for the full ranges in C and D have slopes of $-2.25 \times 10^{-3} \text{ s}^{-1}$ and $-2.64 \times 10^{-3} \text{ s}^{-1}$, corresponding to λ -values of 1.0 and 1.2 in Eq. 5.2. The slopes of the final sections of the two curves both correspond to $\lambda=3$, showing that all borazine impinging on the enclosed Rh is consumed in the final stages. The blue circles in (C) and (D) are the areas numerically calculated using Eq. 5.4 with finite capture zone widths of $w = 0.8 \text{ nm}$ and 0.1 nm respectively

5.4 Discussion

The conclusion that the capture zone has a width in the order of 1 nm at 865 K seems to be in conflict with the fit in Fig. 5.3, in which the value of λ corresponds to a large capture zone, larger than that of the enclosed Rh terrace and even including part of the Rh surface on another terrace. A possible explanation would be that the higher sample temperature at which the experiment shown in Fig. 5.3. was performed makes the decomposition of borazine possible at the bare Rh, while at 865 K an edge of *h*-BN of a step of Rh may be needed for the decomposition of borazine. So the B and N supply would be much higher at 978 K.

5.5 Conclusion

In this chapter, the desorption and decomposition of borazine during growth conditions were investigated. From the formation of compact islands, we determined the decomposition temperature of borazine on Rh(111) to be between 762 K and 806 K. Borazine only decomposes on Rh surface, while molecules landing on *h*-BN do not contribute to the growth. From *h*-BN formation at 865 K, we learned that the effective capture zone for borazine molecules is 1 nm or less around the *h*-BN edge. At 978 K, the capture zone is much wider and the B and the N atoms can diffuse to higher or lower Rh terraces. This implies that at 865 K an edge of *h*-BN or a step of Rh may be needed for the decomposition of borazine, while at 978 K borazine can decompose on a Rh terrace.